Int. J. Solids Structures Vol. 22, No. 6, pp. 643–657, 1986
Printed in Great Britain.

0020-7683/86 $3.00+ .00
Pergamon Journals Ltd.

AN EFFICIENT ELASTODYNAMIC INFINITE ELEMENT

R. K. N. D. RAJAPAKSE and P. KARASUDHI
Division of Structural Engineering and Construction, Asian Institute of Technology,
P.O. Box 2754, Bangkok, Thailand

(*Received* 30 *July* 1984; *in revised form* 30 *July* 1985)

Abstract—An efficient elastodynamic infinite element capable of propagating Rayleigh waves and body waves in a homogeneous half-space is presented. The displacement interpolation functions are presented in convenient explicit forms by formulating the infinite element with respect to a spherical coordinate system. The infinite integrals appearing in the impedance matrix of an infinite element are integrated analytically which results in a drastic reduction in computation cost. These infinite elements are used to model the far field of a homogeneous half-space, while the near field is modelled by conventional finite elements. The applicability and accuracy of the proposed scheme are confirmed by solving several examples.

1. INTRODUCTION

The propagation of elastic waves in a semi-infinite media is one of the most interesting and complicated problems in engineering mechanics and seismology. A clear understanding of the concepts and development of efficient solution schemes are extremely important in the soil-structure interaction analysis of complex structures such as nuclear power plants, off-shore platforms, dams, etc. Since the classical work of Lamb[1], solutions have been obtained for various loading configurations including buried sources. A review of early research on this topic has been done by Miklowitz[2]. The mixed boundary value problems associated with vibratory motion of a rigid body have also been considered as reported by Hadjian *et al.*[3]. Approximate analytical solutions have been presented for an elastic foundation vibrating on the surface of an elastic half-space[4] and for the vertical vibrations of an embedded bar[5]. However, application of analytical solution schemes to most of the practical elastodynamic problems results in mixed boundary value problems which are mathematically intractable. Hence during the last two decades several attempts have been made to present efficient numerical schemes to solve elastodynamic problems of semi-infinite media.

The finite element method is considered as the most versatile numerical method to solve complicated problems. Complicated geometries, boundary conditions and material inhomogeneity can be tackled with relative ease. The usual practice in elastostatics is to model the semi-infinite media by a large number of finite elements with the boundary of the mesh placed at a distance where stresses and displacements are negligibly small. Finite element models of this type, although numerically inefficient, yield accurate results for elastostatics. However, in elastodynamics, finite element models with such elementary boundaries violate the radiation phenomenon of propagating waves in the far field and yield spurious solutions. Waas[6] presented an accurate transmitting boundary for plane and axisymmetric problems of a layered stratum underlain by a rigid base, which was later extended to axisymmetric problems under arbitrary loading by Kausel *et al.*[7]. The global-local finite element method developed by Muki and Dong[8–10] has been extended to study elastodynamic problems of an infinite media by Goetschel *et al.*[11] and recently to study elastodynamic problems of a half-space by Avanessian[12]. In the method, the near field was modelled by conventional finite elements, while the remaining field extending to infinity was represented by a set of known functions called global functions.

The use of infinite elements to model the far field of homogeneous infinite domain problems were pioneered by Bettes[13] and Anderson and Ungless[14]. Recently, Rajapakse and Karasudhi[15–17] presented an elastostatic far-field model for multilayered half-spaces

and three different finite element algorithms to compute the stiffness of far-field domains of such multilayered half-spaces. Medina and Penzien[18] presented elastodynamic infinite elements for homogeneous media, where the integrands of the infinite integrals appearing in the impedance matrices consist of oscillating functions of different periods. These infinite integrals were evaluated using an expensive numerical integration scheme. In the present study, the authors present a two-node elastodynamic infinite element capable of propagating surface waves and body waves. By formulating the infinite elements using a spherical coordinate system, it is found that the infinite integrals appearing in the impedance matrix could be integrated analytically, which results in a drastic reduction in computation cost.

2. FINITE ELEMENT FORMULATION

The reference Cartesian (x, y, z), cylindrical (r, θ, z) and spherical (R, θ, ϕ) coordinate systems are as shown in Fig. 1. Since problems under consideration are limited to those having axial symmetry subjected to nonaxisymmetric loading, the applied forces and displacements could be decomposed into harmonics of the angular coordinate θ. The displacements in r, θ, z directions could be expressed, respectively, as follows:

$$u_r(r, \theta, z, t) = \sum_{n=0}^{\infty} u_{rn}(r, z, t) \cos n\theta + \sum_{n=0}^{\infty} \bar{u}_{rn}(r, z, t) \sin n\theta, \tag{1}$$

$$u_\theta(r, \theta, z, t) = -\sum_{n=0}^{\infty} u_{\theta n}(r, z, t) \sin n\theta + \sum_{n=0}^{\infty} \bar{u}_{\theta n}(r, z, t) \cos n\theta, \tag{2}$$

$$u_z(r, \theta, z, t) = \sum_{n=0}^{\infty} u_{zn}(r, z, t) \cos n\theta + \sum_{n=0}^{\infty} \bar{u}_{zn}(r, z, t) \sin n\theta, \tag{3}$$

where $u_{rn}, u_{\theta n}, u_{zn}$ denote symmetric components of displacement, and $\bar{u}_{rn}, \bar{u}_{\theta n}, \bar{u}_{zn}$ denote antisymmetric components of displacement. The most important advantage of decomposing into harmonics of angle θ is the reduction of the original three-dimensional problem into a two-dimensional problem. Thus a finite element discretization of a continuum results in elements of a toroidal shape symmetrical with respect to the z axis. The applied forces in r, θ and z directions could also be expanded similarly. Without loss of generality, antisymmetric components appearing in eqns (1)–(3) could be dropped, and in what follows, only symmetric components are considered. Formulation corresponding to antisymmetric components could be obtained from that of symmetric components by simply replacing $\cos n\theta$ by $\sin n\theta$ and $-\sin n\theta$ by $\cos n\theta$.

In a general three-dimensional elastodynamic problem the displacement vector $\mathbf{u}(r, \theta, z, t)$ at a point within an element e having m nodes could be approximated by the

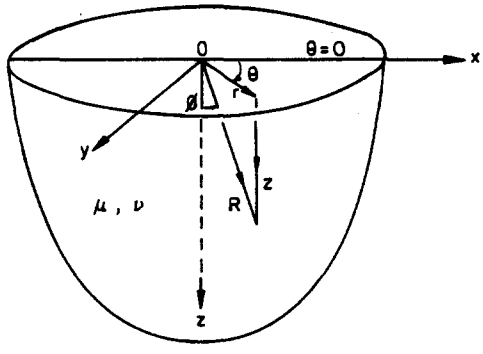

Fig. 1. Half-space with Cartesian coordinates (x, y, z), cylindrical coordinates (r, θ, z) and spherical coordinates (R, θ, ϕ).

harmonics of nodal displacement vector $\mathbf{q}_n^e(t)$ as

$$\mathbf{u}(r,\theta,z,t)=\begin{Bmatrix}u_r(r,\theta,z,t)\\u_z(r,\theta,z,t)\\u_\theta(r,\theta,z,t)\end{Bmatrix}=\sum_{n=0}^{\infty}[N]_n\mathbf{q}_n^e(t), \tag{4}$$

where $[N]_n$ is the displacement interpolation function matrix corresponding to the nth harmonic and defined as

$$[N]_n=\begin{bmatrix}\mathbf{N}^{rn}\cos n\theta & \mathbf{0} & \mathbf{0}\\ \mathbf{0} & \mathbf{N}^{zn}\cos n\theta & \mathbf{0}\\ \mathbf{0} & \mathbf{0} & -\mathbf{N}^{\theta n}\sin n\theta\end{bmatrix} \tag{5}$$

and

$$\mathbf{N}^{rn}=\langle N_1^{rn}N_2^{rn}\cdots N_i^{rn}\cdots N_m^{rn}\rangle, \tag{6}$$

$$\mathbf{N}^{zn}=\langle N_1^{zn}N_2^{zn}\cdots N_i^{zn}\cdots N_m^{zn}\rangle, \tag{7}$$

$$\mathbf{N}^{\theta n}=\langle N_1^{\theta n}N_2^{\theta n}\cdots N_i^{\theta n}\cdots N_m^{\theta n}\rangle, \tag{8}$$

$$\mathbf{q}_n^e(t)=\begin{Bmatrix}\mathbf{q}_{rn}^e(t)\\ \mathbf{q}_{zn}^e(t)\\ \mathbf{q}_{\theta n}^e(t)\end{Bmatrix}, \tag{9}$$

$$\mathbf{q}_{rn}^e(t)=\begin{Bmatrix}u_{rn}^1(t)\\ \vdots\\ u_{rn}^m(t)\end{Bmatrix},\qquad \mathbf{q}_{zn}^e(t)=\begin{Bmatrix}u_{zn}^1(t)\\ \vdots\\ u_{zn}^m(t)\end{Bmatrix},\qquad \mathbf{q}_{\theta n}^e(t)=\begin{Bmatrix}u_{\theta n}^1(t)\\ \vdots\\ u_{\theta n}^m(t)\end{Bmatrix}. \tag{10}$$

In eqns (6)–(8), N_i^{rn}, $N_i^{\theta n}$ and N_i^{zn} denote interpolation functions corresponding to the nth harmonic of displacements in r, θ and z directions, respectively, for node i.

The global nodal displacement vector $\mathbf{u}^e(t)$ of an element e is expressed as

$$\mathbf{u}^e(t)=\sum_{n=0}^{\infty}[Q]_n\mathbf{q}_n^e(t), \tag{11}$$

where $[Q]_n$ is a $3m\times 3m$ matrix defined as

$$[Q]_n=\begin{bmatrix}[Q]_{1n} & & 0\\ & [Q]_{1n} & \\ 0 & & [Q]_{2n}\end{bmatrix}, \tag{12}$$

in which

$$[Q]_{1n}=\begin{bmatrix}\cos n\theta & & 0\\ & \ddots & \\ 0 & & \cos n\theta\end{bmatrix}_{m\times m},\qquad [Q]_{2n}=\begin{bmatrix}-\sin n\theta & & 0\\ & \ddots & \\ 0 & & -\sin n\theta\end{bmatrix}_{m\times m} \tag{13}$$

The strain vector $\boldsymbol{\varepsilon}$ of an element can be expressed in terms of the harmonics of nodal displacements as

$$\boldsymbol{\varepsilon}(r,\theta,z,t)=\sum_{n=0}^{\infty}[B]_n\mathbf{q}_n^e(t). \tag{14}$$

The relationship between the stress vector σ and the strain vector ε can be expressed as

$$\sigma = [D]\varepsilon. \tag{15}$$

In eqn (15), $[D]$ is the constitutive matrix for the material.

The equation of motion for each harmonic n is[17]

$$[M]_n\ddot{\mathbf{q}}_n + [C]_n\dot{\mathbf{q}}_n + [K]_n\mathbf{q}_n = \mathbf{p}_n \qquad (n = 0, \ldots, \infty) \tag{16}$$

where

$$[M]_n = \sum_e [M]_n^e, \qquad [C]_n = \sum_e [C]_n^e, \qquad [K]_n = \sum_e [K]_n^e, \qquad \mathbf{p}_n = \sum_e \mathbf{p}_n^e. \tag{17}$$

In eqn (16), $[M]_n$, $[C]_n$ and $[K]_n$ denote mass, damping, and stiffness matrices, and $\mathbf{P}_n$ denotes the equivalent nodal force vector of the system. The element mass matrix $[C]_n^e$, stiffness matrix $[K]_n^e$ and equivalent nodal force vector $\mathbf{p}_n^e$ are given by

$$[M]_n^e = \int_{v^e} \rho[N]_n^T[N]_n r \, dr \, dz \, d\theta, \tag{18}$$

$$[C]_n^e = \int_{v^e} c[N]_n^T[N]_n r \, dr \, dz \, d\theta, \tag{19}$$

$$[K]_n^e = \int_{v^e} [B]_n^T[D][B]_n r \, dr \, dz \, d\theta, \tag{20}$$

$$\mathbf{p}_n^e = \int_{v^e} [N]_n^T\mathbf{f}_b r \, dr \, dz \, d\theta + \int_{s^e} [Q]_n^T[Q]_n\mathbf{F}_n^e r \, d\theta. \tag{21}$$

In the above equations, ρ is the material mass density, c is the damping coefficient, $\mathbf{f}_b$ is the body force vector, $\mathbf{F}^e$ is the nodal force vector, v^e is the volume of the element, s^e denotes circular nodal lines of element e, and the superscript T denotes the transpose of a matrix. Application of Fourier transforms to eqn (16) results in

$$\{-\omega^2[M]_n + i\omega[C]_n + [K]_n\}\mathbf{q}_n(\omega) = \mathbf{p}_n(\omega), \tag{22}$$

where $\mathbf{q}_n(\omega)$ and $\mathbf{p}_n(\omega)$ are the Fourier transforms of the nth harmonic component of the nodal displacement vector and the equivalent nodal force vector, respectively. Equation (22) is easier to handle in finite element analysis than eqn (16). A more convenient way of writing eqn (22) is

$$[s(\omega)]_n\mathbf{q}_n(\omega) = \mathbf{p}_n(\omega), \tag{23}$$

where

$$[s(\omega)]_n = -\omega^2[M]_n + i\omega[C]_n + [K]_n \tag{24}$$

is the nth harmonic of the system impedance matrix. Solution of eqn (23) results in $\mathbf{q}_n(\omega)$ and the time domain solution $\mathbf{q}_n(t)$ can be obtained subsequently by applying the inverse Fourier transform formula

$$\mathbf{q}_n(t) = \frac{1}{2\pi}\int_{-\infty}^{\infty} \mathbf{q}_n(\omega)\, e^{i\omega t} \, d\omega. \tag{25}$$

3. ELASTODYNAMIC FAR-FIELD BEHAVIOUR

Displacement interpolation functions of an elastodynamic infinite element should ensure that the displacements, within an element, decrease with distance and consist of functions representing out-going waves. A logical way of determining the displacement interpolation functions of an infinite element is to investigate the far-field behaviour of analytical solutions of representative problems.

Forced torsional oscillation of a homogeneous half-space represents one of the simplest wave propagation problems associated with semi-infinite media due to the existence of only one type of wave. A homogeneous half-space subjected to a dynamic torque distributed over a circular area is considered. Assuming steady state excitation of the form $e^{i\omega t}$, it can be shown that the only nonvanishing displacement in the θ direction is given by

$$e^{i\omega t}\, u_\theta(r, z; \omega) = \frac{e^{i\omega t}}{\mu} \int_0^\infty \frac{J_1(\xi r) J_2(\xi)}{\sqrt{\xi^2 - k_s^2}}\, e^{-z\sqrt{\xi^2 - k_s^2}}\, d\xi, \tag{26}$$

where μ is the shear modulus, J_1 and J_2 are Bessel functions of the first kind, and k_s is the shear wave number defined as

$$k_s = \omega/\sqrt{\mu/\rho}. \tag{27}$$

By adopting a suitable contour integration in a complex plane, it can be shown that the far-field behaviour of u_θ is as follows:

$$e^{i\omega t}\, u_\theta(R, \phi; \omega) \sim \frac{ik_s^2}{R}\, e^{i(\omega t - k_r R)} \sin\phi + O(R^{-2}). \tag{28}$$

The propagation of elastic waves in an isotropic, homogeneous, semi-infinite solid under general loading involved more complicated solution procedures[1]. The displacements in r, θ, ϕ directions consist of contributions from Rayleigh waves and body waves. Derivation of exact expressions due to each type of wave at an interior point involves complicated contour integrations and leads to expressions which prevent the realization of the main objective of obtaining an efficient elastodynamic infinite element. Therefore, the far-field behaviour of Rayleigh and body waves are obtained from existing solutions.

Sezawa[19] performed a detailed investigation on Rayleigh waves having azimuthal distribution and presented the following expressions for associated displacements in cylindrical coordinates corresponding to the nth harmonic:

$$e^{i\omega t}\, u_{rn}^f(r, z; \omega) = -e^{i\omega t}\, A_n \frac{k_r}{k_p^2} \left\{ e^{-pz} - \frac{2ps}{k_r^2 + s^2}\, e^{-sz} \right\} \frac{\partial H_n^{(2)}(k_r r)}{\partial(k_r r)}, \tag{29}$$

$$e^{i\omega t}\, u_{\theta n}^f(r, z; \omega) = -e^{i\omega t}\, nA_n \frac{k_r}{k_p^2} \left\{ e^{-pz} - \frac{2ps}{k_r^2 + s^2}\, e^{-sz} \right\} \frac{H_n^{(2)}(k_r r)}{(k_r r)}, \tag{30}$$

$$e^{i\omega t}\, u_{zn}^f(r, z; \omega) = -e^{i\omega t}\, A_n \frac{p}{k_p^2} \left\{ e^{-pz} - \frac{2k_r^2}{k_r^2 + s^2}\, e^{-sz} \right\} H_n^{(2)}(k_r r), \tag{31}$$

where k_p is the pressure wave number defined as

$$k_p = \omega/\sqrt{(\lambda + 2\mu)/\rho}. \tag{32}$$

k_r is the Rayleigh wave number determined as the real and positive root from the following frequency equation

$$(2k^2 - k_s^2)^2 - 4k^2\sqrt{(k^2 - k_p^2)(k^2 - k_s^2)} = 0 \tag{33}$$

and p and s are the following:

$$p = \sqrt{k_r^2 - k_p^2}, \qquad s = \sqrt{k_r^2 - k_s^2}. \tag{34}$$

In addition, A_n is an arbitrary constant, $H_m^{(2)}$ a Bessel function of the third kind or simply a Hankel function, the superscript f indicates that the displacements correspond to free surface waves, and λ is a Lamè constant. Medina and Penzien[18] showed that displacements $u_R^b, u_\phi^b, u_\theta^b$ in spherical coordinates corresponding to the propagation of spherically symmetric body waves can be expressed as

$$u_R^b = A_R h_\backslash^{(2)}(k_p R), \tag{35}$$

$$u_\phi^b = A_\phi h_0^{(2)}(k_s R), \tag{36}$$

$$u_\theta^b = A_\theta h_0^{(2)}(k_s R), \tag{37}$$

where $h_m^{(2)}$ is a spherical Bessel function of the third kind, the superscript b denotes that the displacements correspond to body waves, A_R, A_ϕ and A_θ are arbitrary constants to be determined from appropriate boundary conditions.

4. ELASTODYNAMIC INFINITE ELEMENTS

In general elastodynamic problems, each displacement component consists of contributions from surface waves and body waves. Therefore, displacement interpolation functions of elastodynamic infinite elements capable of representing the far field of semi-infinite media should consist of terms corresponding to different possible types of waves. At the same time, the near field of the half-space is modelled by a finite element mesh of hemispherical shape having radius R_0 as shown in Fig. 2 is considered.

4.1. *Torsional vibration of a homogeneous half-space*

In torsional vibration of a homogeneous half-space, surface waves do not exist, and only horizontally polarized shear waves (SH) exist. The R^{-1} far-field behaviour of the nonvanishing displacement u_θ is expressed in eqn (28). However, in the present study, it is proposed to assume an exponential type of decay instead, so that the infinite integrals appearing in impedance matrices could be handled conveniently by analytical means. Thus for symmetric torsional loading which could be expressed by a single harmonic term ($n = 0$), the displacement interpolation function $N_j^{\theta 0}$ for node j could be expressed in terms of the local coordinates (ξ, η) as

$$N_j^{\theta 0} = \mathrm{e}^{-b_0 \xi} L_j(\eta), \tag{38}$$

where the coordinate transformation is of the form

$$R = R_0 + \xi, \tag{39}$$

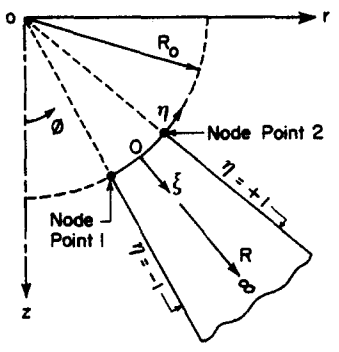

Fig. 2. Two-node elastodynamic infinite element.

$$\phi = \sum_j L_j(\eta)\phi_j \tag{40}$$

and

$$b_0 = (1+i)k_s. \tag{41}$$

The element satisfies compatibility, completeness and is well defined at zero frequency. $L_j(\eta)$ is the Lagrange polynomial corresponding to node j. In evaluating mass and stiffness matrices, infinite integrals with respect to ξ coordinate are of the following form[17]:

$$\int_0^\infty e^{-2b_0\xi}\, d\xi = \frac{1}{2b_0}, \tag{42}$$

$$\int_0^\infty R\, e^{-2b_0\xi}\, d\xi = \frac{R_0}{2b_0} + \frac{1}{4b_0^2}, \tag{43}$$

$$\int_0^\infty R^2\, e^{-2b_0\xi}\, d\xi = \frac{R_0^2}{2b_0} + \frac{R_0}{2b_0^2} + \frac{1}{4b_0^3}. \tag{44}$$

The remaining integration in η direction is performed numerically using the standard Gauss quadrature. It is observed that the integrals in η direction are independent of frequency of excitation and involve simple trigonometric functions and Lagrange polynomials. Thus these integrals can be accurately evaluated by using three integration points in η direction.

4.2. *General vibration of a homogeneous half-space*

The formulation of problems of general vibration of a homogeneous half-space is based on a spherical coordinate system. In such a situation, each displacement u_R, u_ϕ and u_θ consists of a surface wave component and a single body wave component. Equations (29)–(31) present expressions for the Rayleigh wave components. The existence of Bessel functions of the radial coordinates in those equations results in complicated integrals in the impedance matrix, for which convenient closed form expressions are unavailable. The same is true for body wave functions presented in eqns (35)–(37). Thus it is necessary to adopt a simple and logical approximation to replace these Bessel functions enabling analytical integration in the infinite direction. While the true decays of $H_n^{(2)}(y)$ and $h_n^{(2)}(y)$ follow $y^{-1/2}$ and y^{-1} rules, respectively[20], for a large y, it is proposed herein to replace these Bessel functions for a large argument by exponential functions as follows:

$$H_n^{(2)}(y) \to \sqrt{(2/\pi)}\, e^{i\pi(n/2+1/4)}\, e^{-(1+i)y}, \tag{45}$$

$$h_n^{(2)}(y) \to e^{i\pi(n/2+1/2)}\, e^{-(1+i)y}. \tag{46}$$

Accordingly, eqns (29)–(31) and (35)–(37) are approximated by

$$u_{rn}^f(R,\phi) = -A_n\alpha_n\{e^{-pR\cos\phi} - \lambda_1\, e^{-sR\cos\phi}\}\, e^{-(1+i)k_rR\sin\phi}, \tag{47}$$

$$u_{\theta n}^f(R,\phi) \sim n\gamma_n\{e^{-pR\cos\phi} - \lambda_1\, e^{-sR\cos\phi}\}\, e^{-(1+i)k_rR\sin\phi}, \tag{48}$$

$$u_{zn}^f(R,\phi) = -A_n\beta_n\{e^{-pR\cos\phi} - \lambda_2\, e^{-sR\cos\phi}\}\, e^{-(1+i)k_rR\sin\phi}, \tag{49}$$

$$u_R^b = A'_R\, e^{-(1+i)k_pR}, \tag{50}$$

$$u_\theta^b = A'_\theta\, e^{-(1+i)k_pR}, \tag{51}$$

$$u_\phi^b = A'_\phi\, e^{-(1+i)k_sR}, \tag{52}$$

where

$$\alpha_n = (k_r/2k_p^2)\{e^{i\pi[1/4+(n-1)/2]} - e^{i\pi[1/4+(n+1)/2]}\}, \tag{53}$$

$$\gamma_n = (k_r/k_p^2)\, e^{i\pi(1/4+n/2)}, \tag{54}$$

$$\beta_n = (p/k_p^2)\, e^{i\pi(1/4+n/2)}, \tag{55}$$

$$\lambda_1 = 2ps/(k_r^2+s^2), \tag{56}$$

$$\lambda_2 = 2k_r^2/(k_r^2+s^2), \tag{57}$$

and A_n, A'_R, A'_ϕ and A'_θ are arbitrary constants. Equations (47)–(52) would serve as the basis for the development of displacement interpolation functions of an infinite element in the present study. A similar far-field model of an exponential decay was proposed by Medina and Penzien[18] for elastodynamic infinite elements.

Rayleigh wave displacements u^f_{rn}, $u^f_{\theta n}$ and u^f_{zn} in cylindrical coordinates can be transformed into the corresponding spherical components u^f_{Rn}, $u^f_{\theta n}$ and $u^f_{\phi n}$.

Thus each harmonic of displacement in R, ϕ, θ directions can be written as follows:

$$u_{Rn} = u^f_{Rn} + u^b_R, \tag{58}$$

$$u_{\phi n} = u^f_{\phi n} + u^b_\phi, \tag{59}$$

$$u_{\theta n} = u^f_{\theta n} + u^b_\theta, \tag{60}$$

Substitution of Rayleigh and body wave components from eqns (47)–(52) into eqns (58)–(60) show that each displacement expression has two unknown constants. By considering a two node infinite element as shown in Fig. 2 it is possible to express these two unknown constants in terms of the displacements and spherical coordinates of the nodes. The coordinate transformation is the same as that in the torsion problem, i.e. according to eqns (39) and (40). Consider the nth harmonic of the displacement in R direction. In view of eqn (58), the following relationship can be established for the two nodes:

$$\begin{Bmatrix} u^1_{Rn} \\ u^2_{Rn} \end{Bmatrix} = \begin{bmatrix} (J_R)_{11} & (J_R)_{12} \\ (J_R)_{21} & (J_R)_{22} \end{bmatrix} \begin{Bmatrix} A^e_{Rn} \\ A^e_R \end{Bmatrix}. \tag{61}$$

In eqn (61), u^1_{Rn} and u^2_{Rn} are the nth harmonics of the nodal displacements in R direction at node point 1 and node point 2, respectively, and A^e_{Rn} and A^e_R are arbitrary constants associated with far-field displacements for an element e.

Inverting eqn (61),

$$\begin{Bmatrix} A^e_{Rn} \\ A^e_R \end{Bmatrix} = \frac{1}{\Delta^e_R} \begin{bmatrix} (J_R)_{22} & -(J_R)_{12} \\ -(J_R)_{21} & (J_R)_{11} \end{bmatrix} \begin{Bmatrix} u^1_{Rn} \\ u^2_{Rn} \end{Bmatrix}, \tag{62}$$

where

$$\Delta^e_R = (J_R)_{11}(J_R)_{22} - (J_R)_{12}(J_R)_{21}. \tag{63}$$

In view of eqn (62) and after substituting appropriate displacements from eqns (47)–(52), the displacement u_{Rn} of a point inside an element e can be expressed in terms of its nodal values as

$$u_{Rn} = \sum_{j=1}^{2} N_j^{Rn}(\phi, R) u^j_{Rn}, \tag{64}$$

where

$$N_j^{Rn}(\phi, R) = \sum_{m=1}^{3} A_{mj}(\phi)\, \mathrm{e}^{-a_m R}. \tag{65}$$

Following the identical procedure, displacements $u_{\phi n}$ and $u_{\theta n}$ could also be expressed in terms of the nodal values of the element e as

$$u_{\phi n} = \sum_{j=1}^{2} N_j^{\phi n}(\phi, R) u_{\phi n}^j, \tag{66}$$

$$u_{\theta n} = \sum_{j=1}^{2} N_j^{\theta n}(\phi, R) u_{\theta n}^j, \tag{67}$$

where

$$N_j^{\phi n}(\phi, R) = \sum_{m=1}^{3} B_{mj}(\phi)\, \mathrm{e}^{-b_m R}, \tag{68}$$

$$N_j^{\theta n}(\phi, R) = \sum_{m=1}^{3} C_{mj}(\phi)\, \mathrm{e}^{-c_m R}. \tag{69}$$

The terms A_{mj}, B_{mj}, C_{mj}, a_m, b_m and c_m are presented explicitly in the Appendix for the general vibration case.

In evaluating mass and stiffness matrices infinite integrals with respect to R are of the form[17]

$$\int_{R_0}^{\infty} R^k\, \mathrm{e}^{-g_{ml} R}\, \mathrm{d}R \qquad (k = 0, 1, 2). \tag{70}$$

Since g_{ml} is independent of R, integrals in eqn (70) can be easily integrated exactly as follows:

$$\int_{R_0}^{\infty} \mathrm{e}^{-g_{ml} R}\, \mathrm{d}R = \mathrm{e}^{-g_{ml} R_0}/g_{ml}, \tag{71}$$

$$\int_{R_0}^{\infty} R\, \mathrm{e}^{-g_{ml} R}\, \mathrm{d}R = \mathrm{e}^{-g_{ml} R_0}\left[\frac{R_0}{g_{ml}} + \frac{1}{(g_{ml})^2}\right], \tag{72}$$

$$\int_{R_0}^{\infty} R^2\, \mathrm{e}^{-g_{ml} R}\, \mathrm{d}R = \mathrm{e}^{-g_{ml} R_0}\left[\frac{R_0^2}{g_{ml}} + \frac{2R_0}{g_{ml}^2} + \frac{2}{g_{ml}^3}\right]. \tag{73}$$

What remain are integrals in η direction. These can be accurately computed by using the standard Gauss quadrature formula.

Since the computation of the infinite element impedance matrix is in terms of spherical coordinates, it is necessary to perform the following transformation before assembling into the global impedance in terms of cylindrical coordinates:

$$[s(\omega)]_n^e = [A]^T [\hat{s}(\omega)]_n^e [A], \tag{74}$$

where $[s(\omega)]_n^e$ and $[\hat{s}(\omega)]_n^e$ are impedance matrices based on cylindrical and spherical coordinates, respectively, and $[A]$ is the coordinate transformation matrix from cylindrical to spherical[17].

5. DISCUSSION OF RESULTS AND CONCLUSIONS

In solving elastodynamic problems using the finite element method, special attention has to be paid to the dimensions of elements. Previous studies[3, 21] indicate that to adequately transmit a given frequency through the model, the dimensions of a finite element should be kept within a certain limit of the smallest wavelength of the propagating waves. In the present study, wherever possible, nine-node finite elements with 3×3 Gauss quadrature are used to model the near field, and the element size is kept within 1/4 of the shear wavelength.

A rigid circular plate subjected to harmonic torsion is analysed using the mesh shown in Fig. 3(a) and the results are given in Fig. 3(b). It could be easily seen that the mesh shown in Fig. 3(a) gives reasonably accurate results within the dimensionless frequency range 0–3.0. However, as the frequency increases, results deviate more from the analytical solution, since the dimensions of some elements are exceeding the allowable limit specified previously. The mesh shown in Fig. 3(c), which consists of finite elements satisfying the size requirement throughout the dimensionless frequency range 0–6.0, gives very accurate results as shown by Fig. 3(d). The torsional response of an embedded hemisphere is analysed by using the mesh shown in Fig. 4(a). By keeping $R_0 = 1.75a$, all finite elements satisfy the size requirement prescribed previously and the results are found to be very accurate as shown by Fig. 4(b). If $R_0 = 2.2a$, then for high frequencies results are found

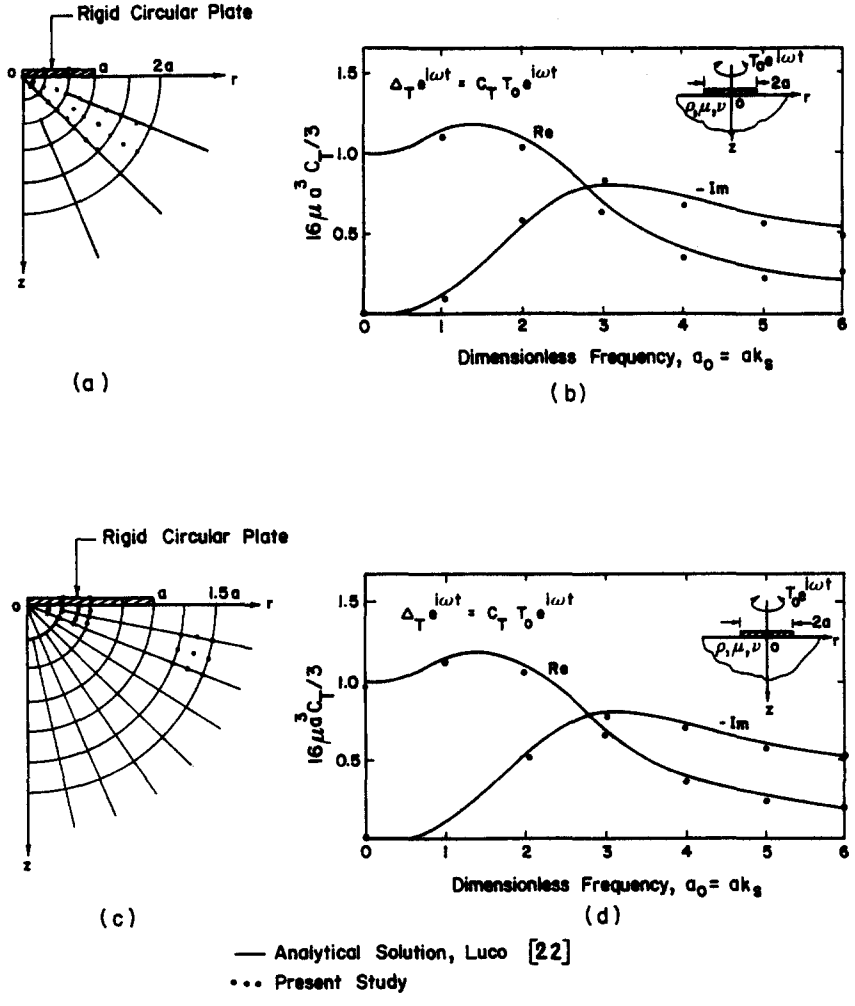

Fig. 3. Torsional compliance, $C_T = \Delta_T/T_0$, of rigid circular plate bonded to homogeneous half-space and subjected to harmonic torque; element mesh (a) giving results in (b) and element mesh (c) giving results in (d).

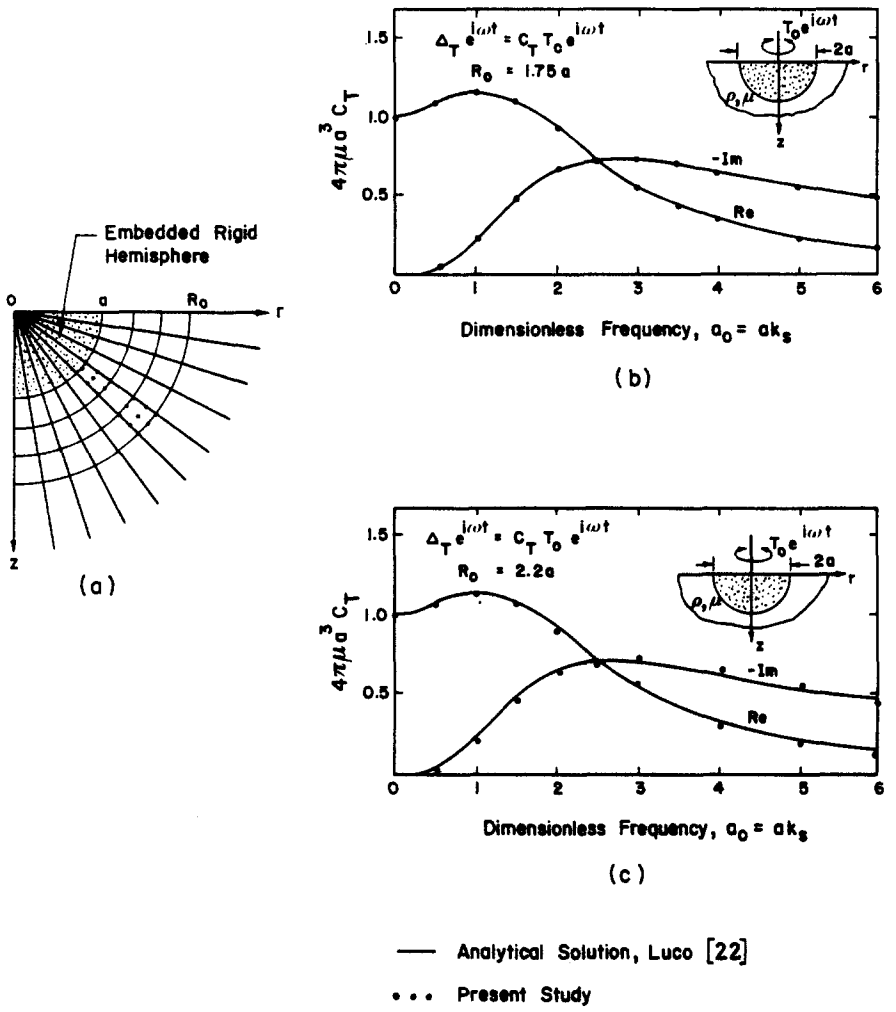

Fig. 4. Torsional compliance, $C_T = \Delta_T/T_0$, of rigid hemisphere embedded in homogeneous half-space.

to be deviating slightly from the analytical solution, since dimensions of some finite elements exceed the allowable maximum dimension specified previously.

Next the two-node elastodynamic infinite element is used to solve symmetric and asymmetric vibration problems associated with a rigid circular plate. The present two-node elastodynamic infinite element violates compatibility and is undefined at zero frequency. However, for zero frequency, the authors have presented three different simple and highly accurate algorithms[16, 17]. In a separate study[17], various mesh configurations have been studied in detail by solving the harmonic uniform vertical pressure problem considered by Sung[23]. Figures 5 and 6 show the results obtained for vertical, lateral and rocking vibration problems. The analytical results[24, 25] are based on the smooth footing assumption. However, in finite element analysis, one obtains perfect bonding between the plate and half-space unless special elements are employed to simulate a smooth interface. Nevertheless, the plate compliances under smooth and rough interface conditions are reasonably close to each other as seen in Figs. 5 and 6. For low frequencies ($a_0 < 0.75$) results were obtained by placing the finite element boundary at a distance equal to 6 times the plate radius. However, this does not cause any penalty on computational cost since the allowable maximum dimensions of the near-field elements are quite large for low frequencies.

The main advantages of the infinite elements developed are that the displacement shape functions are presented explicitly and that the infinite integrals appearing in the

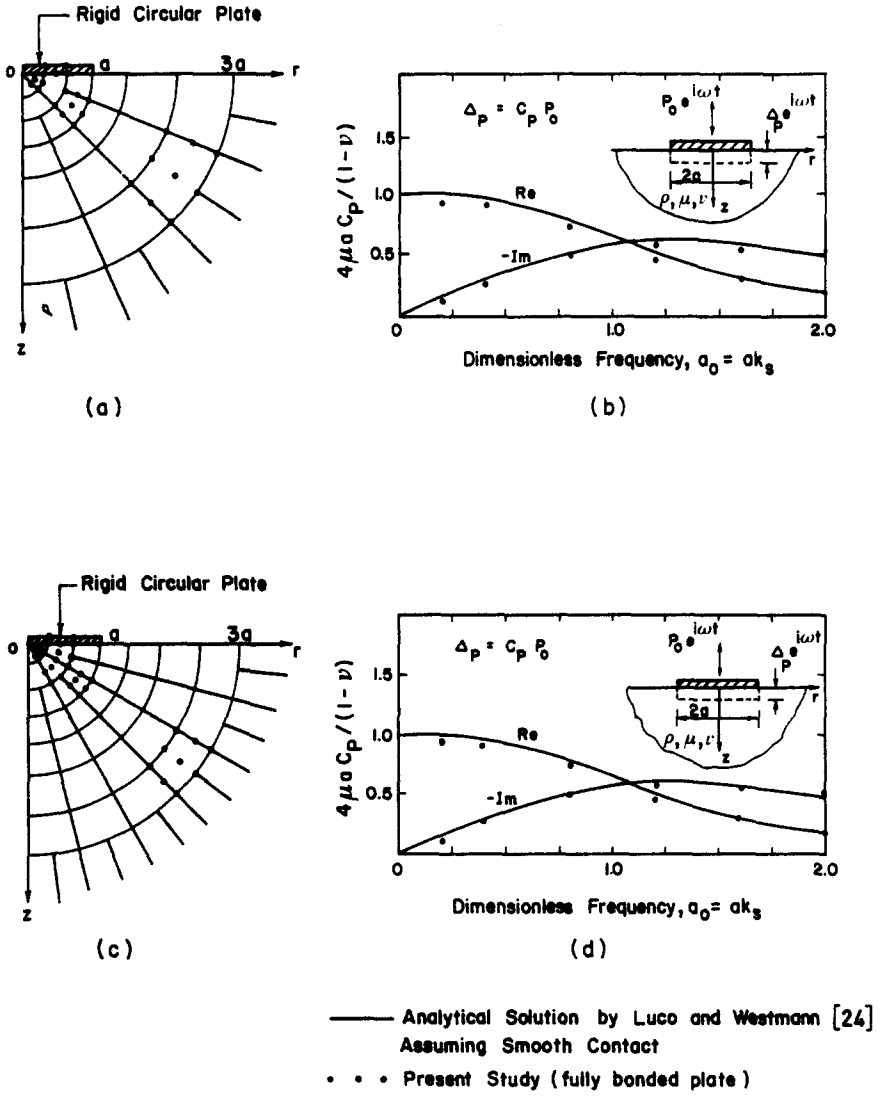

Fig. 5. Vertical compliance, $C_P = \Delta_P/P_0$, of rigid circular plate bonded to homogeneous half-space ($\nu = 1/3$) and subjected to symmetrical vertical load; element mesh (a) giving results in (b), and element mesh (c) giving results in (d).

impedance matrix of an infinite element are easily integrated by analytical means. The latter makes the element computationally very attractive and extremely accurate. These factors make the present element more efficient than those reported in Ref. [18].

A main purpose of this study is to develop efficient infinite elements to model the elastic far field of a homogeneous half-space. The developed algorithm has almost unlimited capacity to handle any vibration problems such as soil-structure interaction, crack, scattering problems, etc. In order to enhance the computational efficiency further, the authors are refining the algorithm by using a certain number of horizontal infinite elements near the surface of the half-space. The concept is similar to that employed very successfully in elastostatic problems[16]. The dynamic results obtained so far for problems of a cylindrical body partially embedded in the half-space have been very promising and will appear in a future publication.

In conclusion, simple and efficient elastodynamic elements capable of propagating surface and body waves are presented in this study to model the elastic far field of a homogeneous half-space. The applicability and accuracy of the elements are confirmed by numerical solutions.

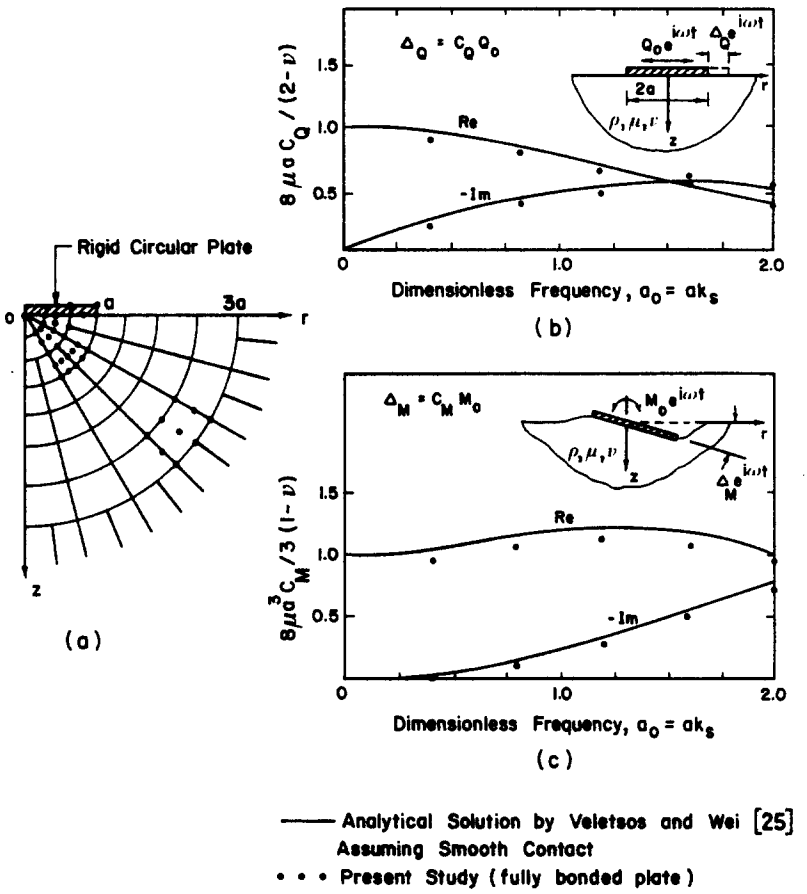

Fig. 6. Rigid circular plate bonded to homogeneous half-space ($\nu = 1/3$); (a) element mesh, (b) horizontal compliance C_Q and (c) rocking compliance C_M.

Acknowledgements—The present paper is based in part on the dissertation by the first author[17], which was submitted in partial fulfilment of the requirements for the degree of Doctor of Engineering at the Asian Institute of Technology. The authors are indebted to the Dissertation External Examiner, Professor Anestis S. Veletsos of Rice University, for his review comments.

REFERENCES

1. H. Lamb, On the propagation of tremors over the surface of an elastic solid. *Phil. Trans. R. Soc. London* **A203,** 1 (1904).
2. J. Miklowitz, Recent developments in elastic wave propagation. *Appl. Mech. Rev.* **13,** 865 (1960).
3. A. H. Hadjian, J. E. Luco and N. C. Tsai, Soil-structure interaction: continuum or finite element method? *Nucl. Engng Design* **31,** 151 (1974).
4. M. Iguchi and J. E. Luco, Dynamic response of flexible rectangular foundations on an elastic half space. *Earthquake Engng Struct. Dynam.* **9,** 239 (1981).
5. G. F. Fowler and G. B. Sinclair, The longitudinal harmonic excitation of a circular bar embedded in an elastic half space. *Int. J. Solids Struct.* **12,** 999 (1978).
6. G. Waas, Dynamic analysis of footing on layered media. Ph.D. thesis, University of California, Berkeley (1972).
7. E. Kausel, J. M. Roësett and G. Waas, Dynamic analysis of footings on layered media. *J. Engng Mech. Div. ASCE* **101,** 679 (1975).
8. R. Muki and S. B. Dong, Some remarks on the use of asymptotic solutions in global-local finite element analysis for an elastic half-space, *Recent Research on Mechanical Behavior of Solids*, p. 55. Univ. Tokyo Press (1979).
9. R. Muki and S. B. Dong, Elastostatic far-field behavior in a layered half-space under surface pressure. *J. Appl. Mech. ASME* **47,** 504 (1980).
10. S. B. Dong, Global-local finite element methods. *State-of-the-Art Survey of Finite Element Methods*, Chap. 14. ASME (1981).
11. D. B. Goetschel, S. B. Dong and R. Muki, A global-local finite element analysis of axisymmetric scattering of elastic waves. *J. Appl. Mech. ASME* **49,** 816 (1982).
12. V. Avanessian, Global-local finite element analysis of pile-soil interaction. M.S. thesis, University of California, Los Angeles (1980).

13. P. Bettes, Infinite elements. *Int. J. Numer. Methods Engng* **11**, 53 (1977).
14. D. L. Anderson and R. F. Ungless, Infinite finite elements. Presented at the International Symposium on Innovative Numerical Analysis and Applications in Engineering Science, Paris, May 1977.
15. R. K. N. D. Rajapakse and P. Karasudhi, Infinite elements for elastostatics of half spaces. *Proceedings of the 4th ASCE-EMD Specialty Conference*, 1983, p. 835.
16. R. K. N. D. Rajapakse and P. Karasudhi, Elastostatic infinite elements for layered half spaces. *J. Engng Mech. ASCE* **111**, 1144 (1985).
17. R. K. N. D. Rajapakse, Appropriate infinite elements for elastostatics and elastodynamics of half spaces. D. Engng Dissertation, Asian Institute of Technology, Bangkok, Thailand (1983).
18. F. Medina and J. Penzien, Infinite elements for elastodynamics. *Earthquake Engng Struct. Dynam.* **10**, 699 (1982).
19. K. Sezawa, Further studies on Rayleigh waves having some azimuthal distributions. *Earthquake Res. Inst. Bull.* **6**, 1 (1929).
20. M. Abramowitz and I. A. Stegun, *Handbook of Mathematical Functions*, 3rd Edn. Dover, New York (1972).
21. S. Gupta, J. Penzien, T. W. Lin and C. S. Yeh, Three-dimensional hybrid modelling of soil-structure interaction. *Earthquake Engng Struct. Dynam.* **10**, 69 (1982).
22. J. E. Luco, Torsional response of structures for SH waves; the case of hemispherical foundations. *Bull. Seismol. Soc. Am.* **66**, 109 (1976).
23. T. Y. Sung, Vibrations in semi-infinite solids due to periodic surface loadings. *Symposium on Dynamic Testing of Soils, ASTM, Special Technical Publication* **156**, 35 (1953).
24. J. E. Luco and R. A. Westmann, Dynamic response of circular footings. *J. Engng Mech. Div. ASCE* **97**, 1381 (1971).
25. A. S. Veletsos and Y. T. Wei, Lateral and rocking vibrations of footings. *J. Soil Mech. Found. Div. ASCE* **97**, 1227 (1971).

APPENDIX

The following are associated with the displacement shape functions:

$$(J_R)_{11} = e^{-(1+i)k_r R_0 \sin\phi_1}\{(\beta_n \cos\phi_1 - \alpha_n \sin\phi_1)\, e^{-pR_0\cos\phi_1} + (\alpha_n\lambda_1 \sin\phi_1 - \beta_n\lambda_2 \cos\phi_1)\, e^{-sR_0\cos\phi_1}\}, \quad (75a)$$

$$(J_R)_{12} = (J_R)_{22} = e^{-(1+i)k_R R_0}, \quad (75b)$$

$$(J_R)_{21} = e^{-(1+i)k_r R_0 \sin\phi_2}\{(\beta_n \cos\phi_2 - \alpha_n \sin\phi_2)\, e^{-pR_0\cos\phi_2} + (\alpha_n\lambda_1 \sin\phi_2 - \beta_n\lambda_2 \cos\phi_2)\, e^{-sR_0\cos\phi_1}\}, \quad (75c)$$

$$(J_\phi)_{11} = e^{-(1+i)k_r R_0 \sin\phi_1}\{-(\alpha_n \cos\phi_1 + \beta_n \sin\phi_1)\, e^{-pR_0\cos\phi_1} + (\alpha_n\lambda_1 \cos\phi_1 + \beta_n\lambda_2 \sin\phi_1)\, e^{-sR_0\cos\phi_1}\}, \quad (76a)$$

$$(J_\phi)_{12} = (J_\phi)_{22} = e^{-(1+i)k_s R_0}, \quad (76b)$$

$$(J_\phi)_{21} = e^{-(1+i)k_r R_0 \sin\phi_2}\{-(\alpha_n \cos\phi_2 + \beta_n \sin\phi_2)\, e^{-pR_0\cos\phi_2} + (\alpha_n\lambda_1 \cos\phi_2 + \beta_n\lambda_2 \sin\phi_2)\, e^{-sR_0\cos\phi_2}\}, \quad (76c)$$

$$(J_\theta)_{11} = -\gamma_n(e^{-pR_0\cos\phi_1} - \lambda_1\, e^{-sR_0\cos\phi_1})\, e^{-(1+i)k_r R_0 \sin\phi_1}, \quad (77a)$$

$$(J_\theta)_{12} = (J_\theta)_{22} = e^{-(1+i)k_s R_0}, \quad (77b)$$

$$(J_\theta)_{21} = -\gamma_n(e^{-pR_0\cos\phi_2} - \lambda_1\, e^{-sR_0\cos\phi_2})\, e^{-(1+i)k_r R_0 \sin\phi_2}, \quad (77c)$$

where ϕ_1 and ϕ_2 are values of ϕ at node points 1 and 2, respectively, while other symbols are as previously defined. The terms A_{mj}, B_{mj}, C_{mj}, a_m, b_m and c_m involved in eqns (65), (68) and (69) are as follows:

$$A_{11}(\phi) = [(J_R)_{22}/\Delta_R^c](\beta_n \cos\phi - \alpha_n \sin\phi), \quad (78a)$$

$$A_{21}(\phi) = [(J_R)_{22}/\Delta_R^c](\alpha_n\lambda_1 \sin\phi - \beta_n\lambda_2 \cos\phi), \quad (78b)$$

$$A_{31} = -(J_R)_{21}/\Delta_R^c, \quad (78c)$$

$$A_{12}(\phi) = [-(J_R)_{12}/\Delta_R^c](\beta_n \cos\phi - \alpha_n \sin\phi), \quad (78d)$$

$$A_{22}(\phi) = [-(J_R)_{12}/\Delta_R^c](\alpha_n\lambda_1 \sin\phi - \beta_n\lambda_2 \cos\phi), \quad (78e)$$

$$A_{32} = (J_R)_{11}/\Delta_R^c, \quad (78f)$$

$$B_{11}(\phi) = [-(J_\phi)_{22}/\Delta_\phi^c](\alpha_n \cos\phi + \beta_n \sin\phi), \quad (79a)$$

$$B_{21}(\phi) = [(J_\phi)_{22}/\Delta_\phi^c](\alpha_n\lambda_1 \cos\phi + \beta_n\lambda_2 \sin\phi), \quad (79b)$$

$$B_{31} = -(J_\phi)_{21}/\Delta_\phi^c, \quad (79c)$$

$$B_{12}(\phi) = [(J_\phi)_{12}/\Delta_\phi^c](\alpha_n \cos\phi + \beta_n \sin\phi), \quad (79d)$$

$$B_{22}(\phi) = [-(J_\phi)_{12}/\Delta_\phi^c](\alpha_n\lambda_1 \cos\phi + \beta_n\lambda_2 \sin\phi), \quad (79e)$$

$$B_{32} = (J_\phi)_{11}/\Delta_\phi^c, \quad (79f)$$

$$C_{11} = [-(J_\theta)_{22}/\Delta_\theta^c]\gamma_n, \quad (80a)$$

$$C_{21} = [(J_\theta)_{22}/\Delta_\theta^c]\gamma_n\lambda_1, \quad (80b)$$

$$C_{31} = -(J_\theta)_{21}/\Delta_\theta^c, \quad (80c)$$

$$C_{12} = [(J_\theta)_{12}/\Delta_\theta^c]\gamma_n, \tag{80d}$$

$$C_{22} = [-(J_\theta)_{12}/\Delta_\theta^c]\gamma_n\lambda_1, \tag{80e}$$

$$C_{32} = (J_\theta)_{11}/\Delta_\theta^c, \tag{80f}$$

$$a_1 = (p\cos\phi + k, \sin\phi + ik, \sin\phi), \tag{81a}$$

$$a_2 = (s\cos\phi + k, \sin\phi + ik, \sin\phi), \tag{81b}$$

$$a_3 = (k_p + ik_p), \tag{81c}$$

$$b_1 = a_1, \tag{82a}$$

$$b_2 = a_2, \tag{82b}$$

$$b_3 = (k_s + ik_s), \tag{82c}$$

$$c_1 = (p\cos\phi + k, \sin\phi + ik, \sin\phi), \tag{83a}$$

$$c_2 = (s\cos\phi + k, \sin\phi + ik, \sin\phi), \tag{83b}$$

$$c_3 = (k_s + ik_s), \tag{83c}$$

in which the symbols Δ_R^c, Δ_ϕ^c and Δ_θ^c are as follows:

$$\Delta_R^c = (J_R)_{11}(J_R)_{22} - (J_R)_{12}(J_R)_{21}, \tag{84a}$$

$$\Delta_\phi^c = (J_\phi)_{11}(J_\phi)_{22} - (J_\phi)_{12}(J_\phi)_{21}, \tag{84b}$$

$$\Delta_\theta^c = (J_\theta)_{11}(J_\theta)_{22} - (J_\theta)_{12}(J_\theta)_{21}. \tag{84c}$$